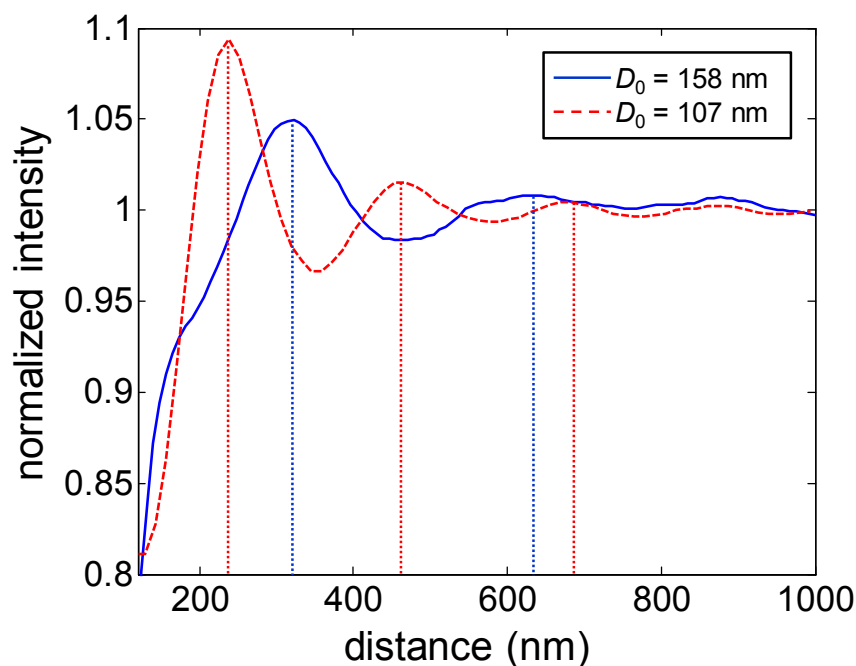


### Radial distribution functions (short range order)

The radial distribution functions for the nanohole arrays (Figure S1) were obtained from image analysis. The plots show that the arrangement of holes on the surface resulting from colloidal lithography is *not* random, but *ordered*, although not over long distances ( $> 1 \mu\text{m}$ ). The average intensity of an image was used for normalization so that a value above one shows correlation. As can be seen, two or even three peaks with a regular period can be identified in the plots. For samples prepared with 158 nm colloids (initial size) the characteristic spacing is 320 nm and for 107 nm colloids (initial size) it is 230 nm. These values did not change when the colloids were treated with  $\text{O}_2$  plasma to reduce hole diameter as expected when the colloid arrangement is fixed.



**Figure S1.** Radial distribution functions obtained from image analysis showing the short-range ordering of the nanoholes. Two peaks can be clearly identified for the larger colloids and three peaks for the smaller. The correlation disappears completely around  $1 \mu\text{m}$ .

### Making small holes by colloids with small initial sizes

As an alternative to shrinking colloids by O<sub>2</sub> plasma, we also prepared plasmonic nanohole arrays simply by using smaller colloids. However, this approach is not as successful for several reasons as explained here. Still, the results are interesting when compared to those in the main text.

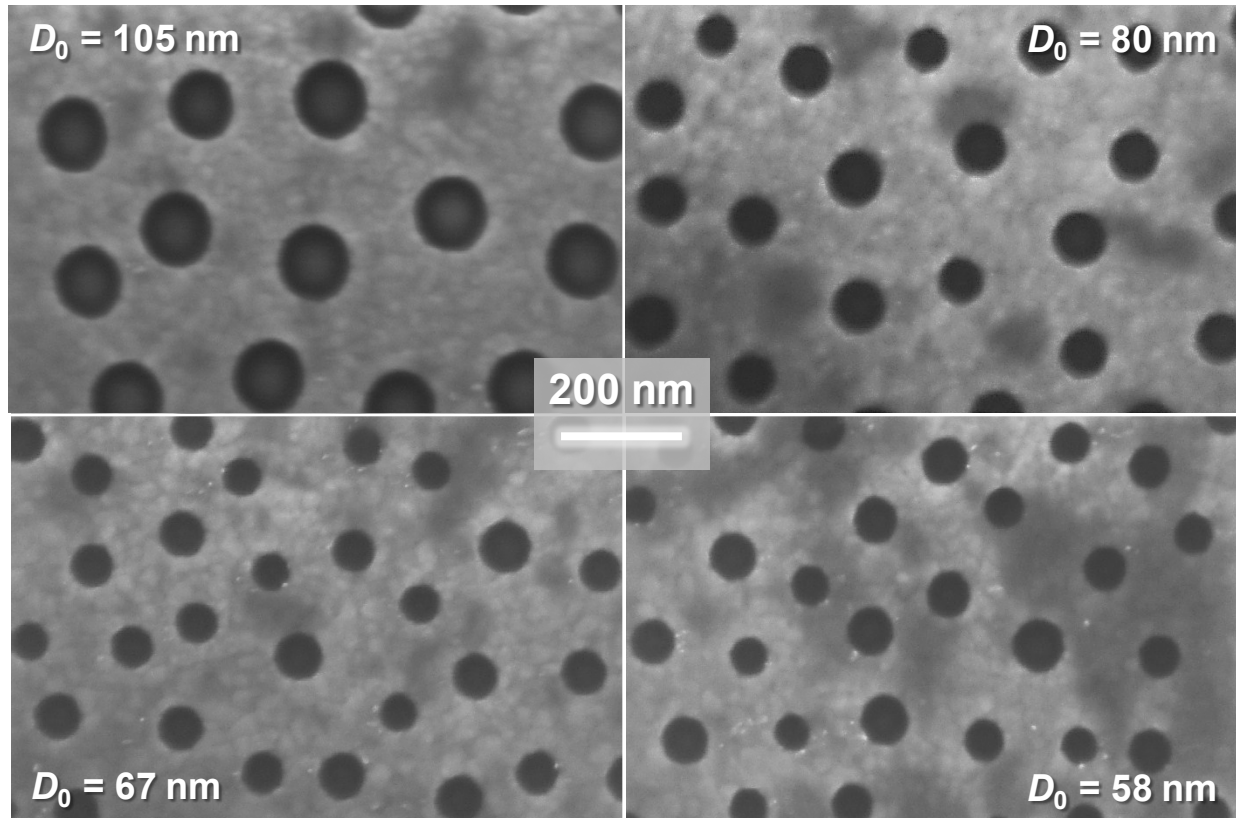


**Figure S2.** Nanoholes prepared directly using small colloids. The given average diameters are those specified for the colloids by the manufacturer.

Images of the nanoholes are shown in Figure S2. It can be seen directly that although these holes are equally nicely circular in shape, they are more closely packed and not as homogenous in size compared with the samples obtained by shrinking colloids. Histograms of the diameters with Gaussian fits are shown in Figure S3. (Data is to be compared with Figure 1C in main text.) We emphasize that here we carefully selected batches of colloids with as *narrow* size distribution as possible. In most cases the heterogeneity in size is even worse. It appears that only for sizes above 100 nm can relatively homogenous diameters (a few nm standard deviation) be acquired from manufacturers.

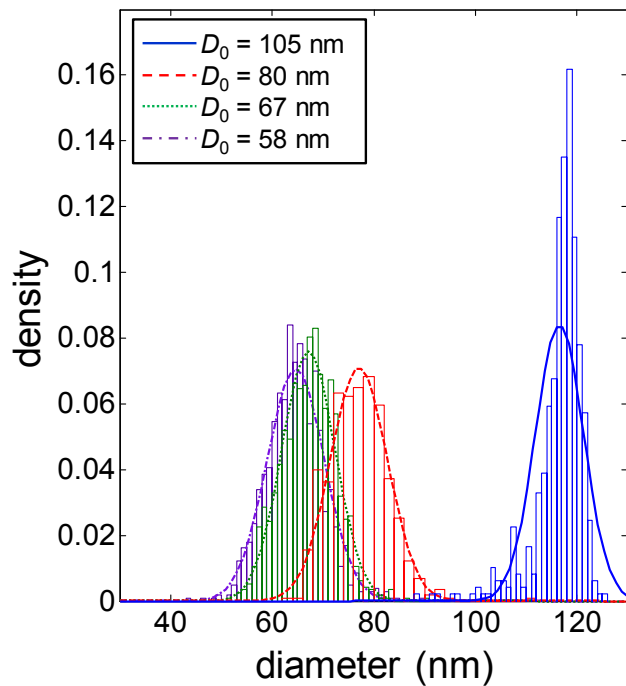


**Figure S3.** Diameter histograms of the holes in Fig. S2. The average diameters in the legend are those specified (for the colloids) by the manufacturer.

Another issue with these nanohole arrays is that due to a lower charge, smaller colloids assemble in more close packed short-range ordered patterns, as shown by the radial distribution functions in Figure S4. The characteristic spacing as represented by the first peak is again evident but clearly reduced for colloids with smaller initial size.

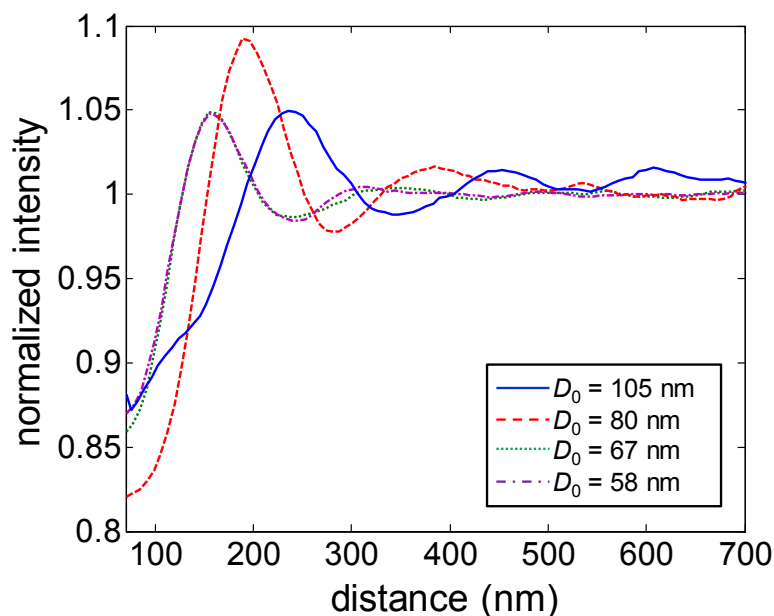


**Figure S4.** Radial distribution functions (obtained from images such as those in Figure S2) for the samples made with colloids with small initial size (no shrinking).

Extinction spectra of the nanohole arrays made by colloids with small diameters are shown in Figure S5. The dip still blueshifts for smaller diameters. However, the extinction peak now also blueshifts, by more than 50 nm as the diameter is reduced by less than 50 nm. This is due to the shorter periodicity

of the arrays (Figure S4) and not due to the smaller diameters. (The grating coupling condition to SP modes predicts a blueshift in agreement with the spectral changes.) The gold thickness was 25 nm for these samples.

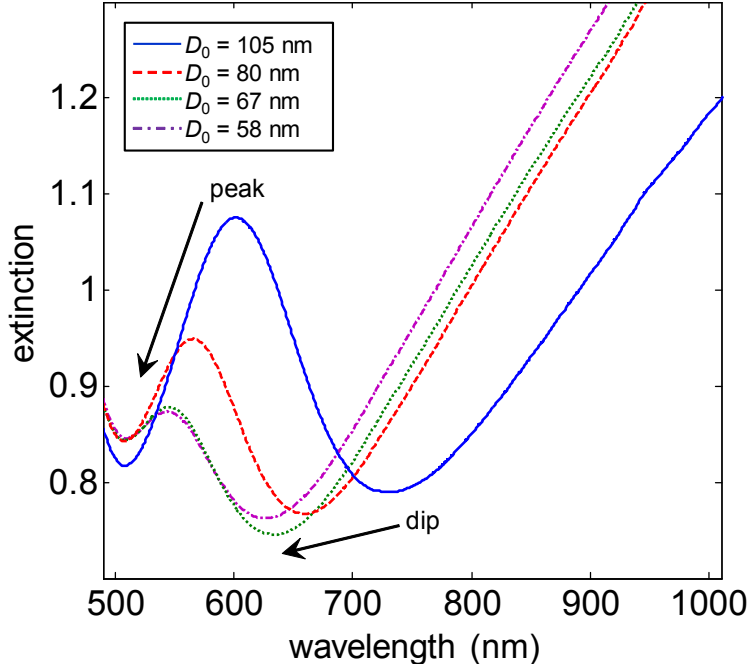


**Figure S5.** Extinction spectra in air of the samples in Figure S2.

### Nanofabrication details

Removal of colloids by tape did not work as well as rubbing the surface, even on samples where there was no alumina layer deposited. However, rubbing required the additional alumina layer since the gold was damaged otherwise (Figure S6). Most likely, other hard materials could also be used instead of alumina.

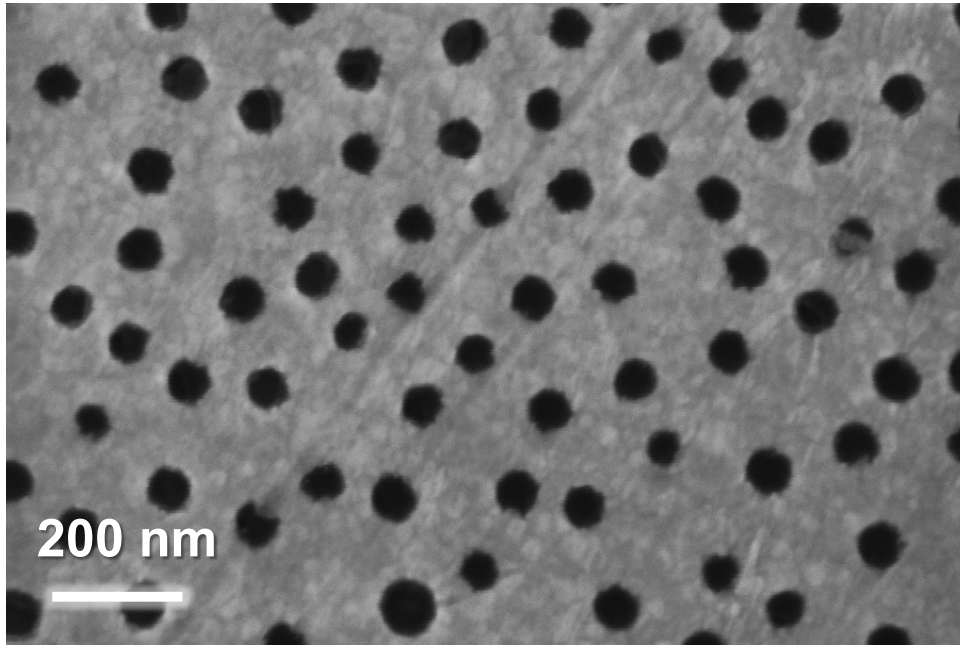


**Figure S6.** Removing colloids by rubbing directly on Au damages the fine structure.

For colloids below 50 nm, removal becomes difficult even when rubbing, at least if the Au film should be as thick as 30 nm. An example is shown in Figure S7, with a significant fraction of stuck colloids.

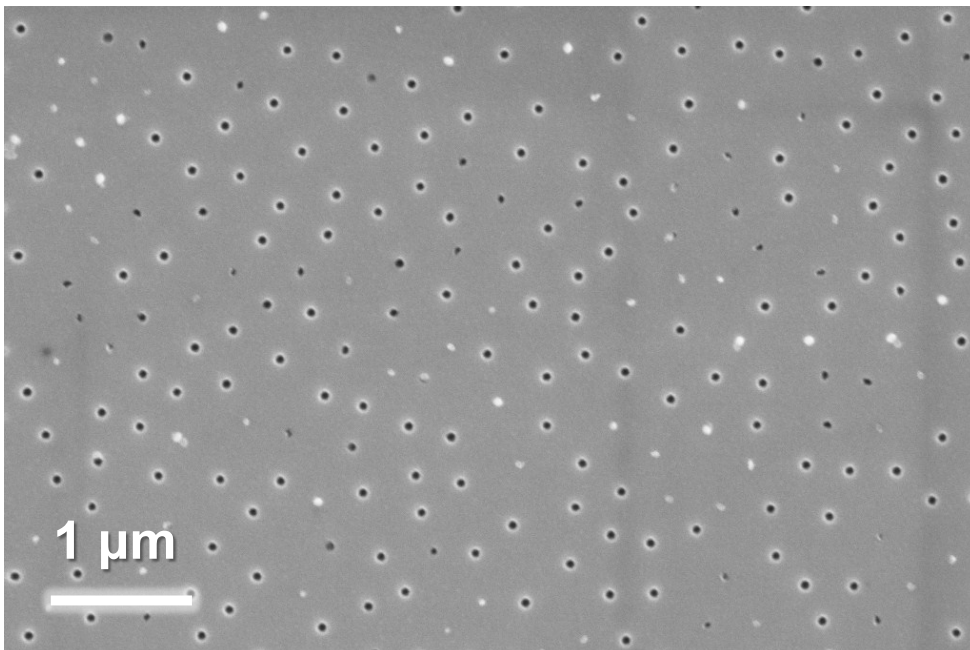


**Figure S7.** Removing colloids smaller than 50 nm (here ~40 nm) becomes difficult after deposition of 30 nm Au + 15 nm Al<sub>2</sub>O<sub>3</sub>.

### Field plot for extinction peak

Figure S8 shows examples of the near field inside the apertures at the extinction *peak* wavelength for the simulated long-range hexagonal arrays with different diameters (Figure 3 in main text). Although there is clearly an enhancement at the edges, as for the extinction dip, several qualitative differences can be identified. The field enhancement is lower and less localized to the void. Further, there is a local minimum above the apertures

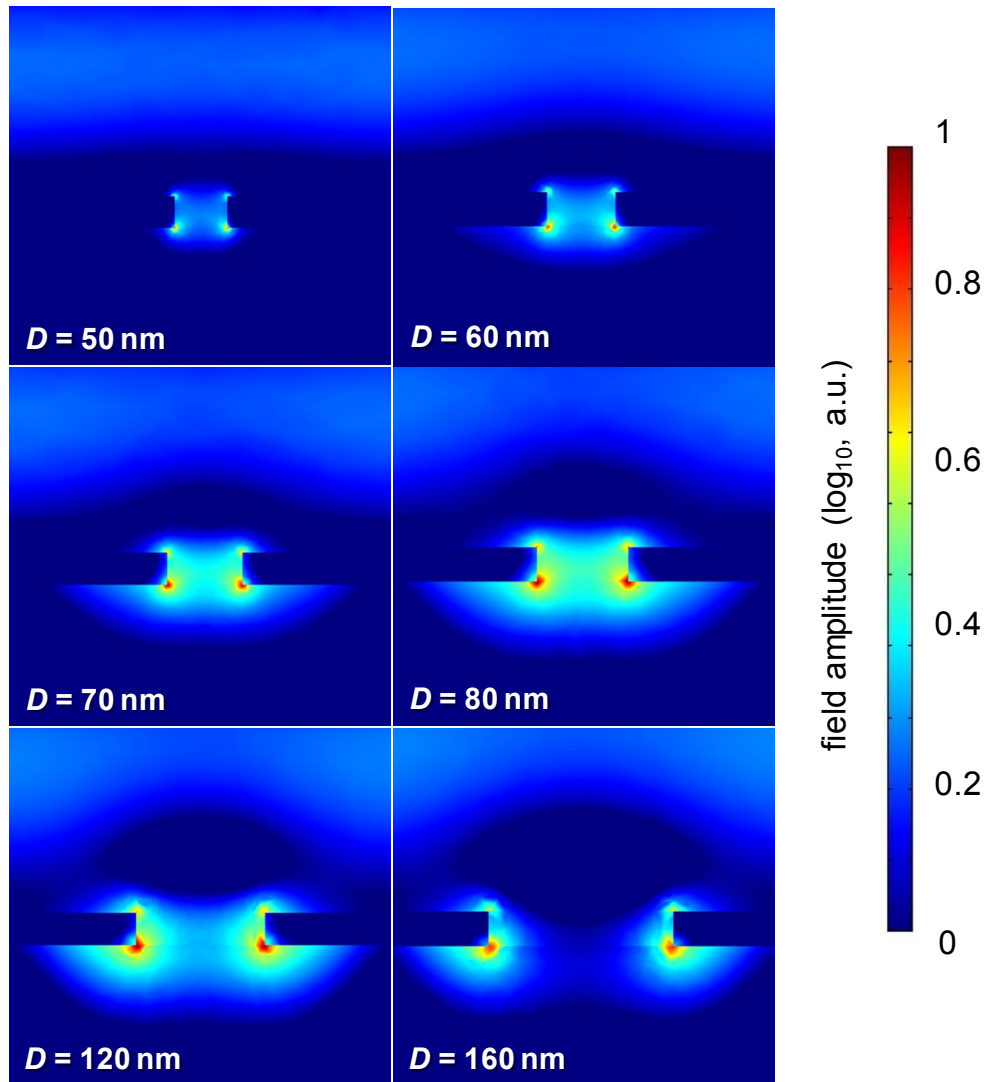


**Figure S8.** Near field plots for the extinction peak for different diameters. To be compared with Figure 3C in main text.

### Thin film extinction

To clarify the influence of the semi-transparent Au film on the extinction spectrum we show the experimental spectrum of a 30 nm Au film (on glass in air) in Figure S9. The extinction was also calculated by Fresnel models and by the same simulation methodology as for the nanohole arrays. There is only a small offset differing between the spectra. The extinction increases for longer wavelengths due to the shorter penetration depth of lower energy photons, which leads to more reflection. For photons at 520 nm or higher energy, the extinction increases due to Au interband transitions. The inclusion of a 1 nm Cr layer (permittivity  $-1.79 + 21.12i$ , non-dispersive in this range) by Fresnel models causes a small overall increase in extinction.

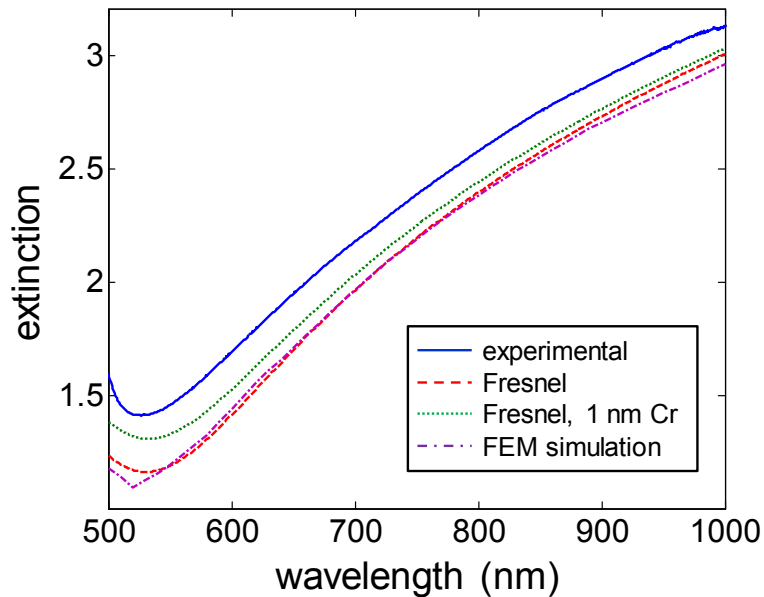


**Figure S9.** Extinction spectra by different methodologies for a 30 nm Au film on glass in air.